HEAT TRANSFER WITH COMBINED MODES

presented at
1994 International Mechanical Engineering Congress and Exposition
Chicago, Illinois
November 6–11, 1994

sponsored by
The Heat Transfer Division, ASME

edited by
D. E. Beasley
Clemson University
K. D. Cole
University of Nebraska

THE AMERICAN SOCIETY OF MECHANICAL ENGINEERS
UNITED ENGINEERING CENTER / 345 EAST 47TH STREET / NEW YORK

HTD-Vol. 299, Heat Transfer With Combined Modes
ASME 1994

TWO-FLUX AND DIFFUSION METHODS FOR RADIATIVE TRANSFER IN COMPOSITE LAYERS

Charles M. Spuckler
Internal Fluid Mechanics Division
NASA Lewis Research Center
Cleveland, Ohio

Robert Siegel
Research Academy
NASA Lewis Research Center
Cleveland, Ohio

ABSTRACT

Radiative transfer is analyzed in composite materials of 2 or 3 layers relative to evaluating ceramic materials being developed for high temperature applications. Some ceramics are partially transparent for radiative transfer. Their refractive indices are greater than one which influences internal reflections and emission. The thermal behavior of single and composite layers has been obtained in the literature by numerical solutions of the radiative transfer equations coupled with heat conduction, and with convection and radiation at the boundaries. Two-flux and diffusion methods are investigated to obtain approximate solutions using much simpler formulations than for exact numerical solutions. The two-flux method yields excellent results for gray and two-band spectral calculations including isotropic scattering. If one layer is optically thick the analysis shows how the diffusion method can be used in that layer and be coupled with the two-flux method in an adjacent layer. Comparisons with numerical solutions of the transfer equations show that this provides accurate temperature distributions and heat fluxes.

NOMENCLATURE

a	absorption coefficient of material in layer, m^{-1}
C_j	coefficients defined in Eq. (17)
CON	integration constant in energy equation, W/m; $\widetilde{CON} = CON/D\sigma T_{g1}^4$
c_o	speed of electromagnetic propagation, m/s
D	thickness of each layer in composite, m
FS,FL	blackbody fraction in small and large frequency bands
G	flux quantity defined in Eq. (1a), W/m^2; $\widetilde{G} = G/\sigma T_{g1}^4$
GS,GL	values of G in bands at small and large frequencies
H	dimensionless convection-radiation parameter, $h/\sigma T_{g1}^3$
h_1,h_2	heat transfer coefficients at boundaries, W/m^2K
k	thermal conductivity, W/mK
K	extinction coefficient, $a + \sigma_s$, m^{-1}
N	conduction-radiation parameter, $k/\sigma T_{g1}^3 D$
NOR	normalization factor
n	refractive index of a layer
q	heat flux, W/m^2; $\tilde{q} = q/\sigma T_{g1}^4$
q_r	radiative heat flux in composite, W/m^2; $\tilde{q}_r = q_r/\sigma T_{g1}^4$
q_r^+,q_r^-	radiative fluxes in + and - x directions, W/m^2
q_r^o	externally incident radiation flux, W/m^2; $\tilde{q}_r^o = q_r^o/\sigma T_{g1}^4$
qS,qL	radiative flux in bands with small and large frequencies
R(n)	function of refractive index defined in Eq. (19)
T	absolute temperature, K
t	dimensionless temperature, T/T_{g1}
T_{g1},T_{g2}	gas temperatures on two sides of composite, K
x	coordinate in a layer, m; X = x/D

Greek symbols

κ	optical coordinate in a layer Kx; κ_D, optical thickness, KD
ν	frequency of radiation
ρ	reflectivity of interface
σ	Stefan-Boltzmann constant, W/m^2K^4
σ_s	scattering coefficient in a layer, m^{-1}
Ω	scattering albedo in a layer, $\sigma_s/(a+\sigma_s) = \sigma_s/K$

Subscripts

a,b...h	the interfaces of a three-layer composite (Fig. 1)
c	value at cutoff frequency
D	based on length D
g	gas on either side of composite
h,s	higher and smaller refractive indices
j	index indicating j th layer in a composite
r	radiative
S,L	spectral bands with small and large frequencies
tot	total heat flux by combined conduction and radiation
ν	frequency dependent quantity
1,2	exterior quantities at outside boundaries (Fig. 1)

INTRODUCTION

The development of ceramic materials for high temperature use is critical for advanced aircraft engines where high thermal efficiency is required. Some ceramics are partially transparent to radiant energy in at least some portions of the wavelength spectrum. For high temperature surroundings, such as in a combustion chamber, infrared

and visible radiation may penetrate into the material and provide internal heating; this can affect internal temperatures of ceramic engine parts and coatings.

For elevated temperature levels, radiant emission within the material can be large. This is especially true for materials with high refractive indices since internal emission depends on the refractive index squared. In addition to internal emission, radiant absorption and scattering, and heat conduction contribute to the energy transfer process. It must be determined when radiative processes become significant, and how large their effects are compared with conditions when materials are assumed opaque. Another aspect is to determine whether partial transparency can help equalize temperatures to reduce thermal stresses, reduce maximum temperatures, and control temperature levels in the material.

In composite layers the refractive indices of the materials produce surface reflections that enter into the radiative transfer. Since emission within a material depends on the square of its refractive index, internal emission can be much larger in a ceramic than in a gas. Radiation leaving through an interface cannot exceed that from a blackbody, and is prevented from doing so by total internal reflections that occur when radiation is passing into a material with a lower refractive index. Internal scattering must be examined as it can influence the temperature distribution for some conditions.

There is an extensive literature on radiative transfer in plane layers originating from the development of theory to study radiation in stellar and the earth's atmospheres. Another important subject studied since the 1920's is radiation by furnace gases. As a result, many investigations of radiation within media have been for gases where the refractive index is very close to one. An important area involving higher refractive indices and hot materials with significant internal emission, is predicting heat treating and cooling of glass plates (Gardon, 1958). The literature has been briefly reviewed in our previous work (Spuckler and Siegel, 1993, 1994). In these papers, temperature distributions and heat flows in partially transmitting materials with high refractive indices are predicted by analyses using the radiative transfer equations coupled with heat conduction. The governing integral equations, including the scattering source function for some of the work, are solved numerically. Each exterior boundary is heated by radiation and convection, and diffuse interface reflections are included. Results are given for a layer with two spectral bands in the absorption coefficient, and for a composite of two gray layers. For use in the development of approximate solutions, the numerical solutions were extended in Siegel and Spuckler (1994) to a three-layer composite including up to three spectral bands in each layer. Isotropic scattering is included. This simulates a ceramic layer with a reinforcing layer, or coatings of other ceramic materials for protection against corrosive atmospheres such as combustion gases. Various amounts of isotropic scattering are included to simulate internal reflections by a granular or reinforcing structure.

The formulation and solution of the exact spectral radiative transfer equations including scattering is rather complicated; hence it is desirable to develop more convenient approximate methods such as the two-flux method if these will yield accurate results. The two-flux equations are given in Sidall (1972), and Siegel and Howell (1992). The two-flux method was shown in Malpica et al. (1986), and Tremante and Malpica (1993) to give accurate results for a gray layer with a refractive index of one between boundaries with specified temperatures. Two-flux and diffusion solutions, and combinations of the two for layers with optically thin and thick spectral bands, were derived in Siegel and Spuckler (1994) for materials with refractive

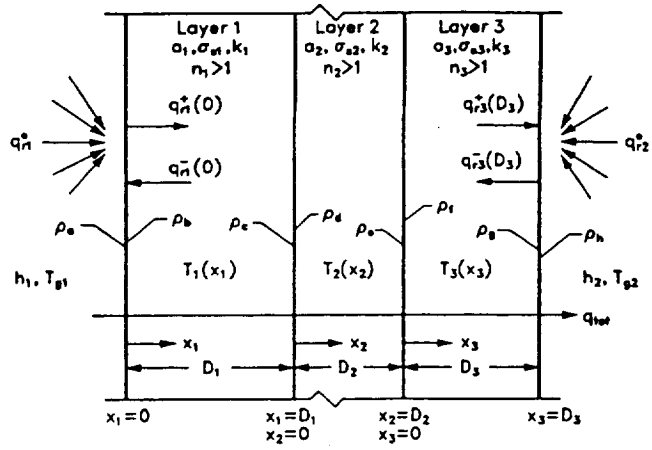

FIG. 1 GEOMETRY AND COORDINATE SYSTEM FOR TWO-FLUX ANALYSIS IN A COMPOSITE OF THREE ABSORBING, EMITTING AND SCATTERING SEMITRANSPARENT LAYERS.

indices larger than one, and for heating conditions such that the boundary temperatures are not specified and must be determined during the solution. These provide a simplified formulation, and were found to be very accurate for a single layer by comparisons with exact solutions. In the present work further analysis is made to treat multilayer composites of materials with refractive indices larger than one. The two-flux method is found to work well for layers with optical thicknesses less than about 20. It is joined here with the diffusion solution for situations where there is an adjacent optically thick layer. This yields excellent results for two band spectral calculations in composite layers, including an optically thick layer, and with isotropic scattering included.

ANALYSIS

The Two-Flux Method for Radiative Transfer in a Three-Layer Gray Composite

A composite layer of absorbing, emitting, and isotropically scattering materials has convection and incident radiation on each of its external boundaries as shown in Fig. 1 for a three-layer region. The two-flux method is developed here to obtain the temperature distribution and heat flux through the composite. To begin the development a three-layer composite of gray materials is considered. Adjacent layers each have a different refractive index. The resulting two-flux relations provide a foundation to analyze a larger number of layers with banded spectral properties. Relations are given for two spectral bands in each layer of a two-layer composite. The two-flux method is also combined with the diffusion method to treat multiple layers with one or more layers being optically thick. Results are compared with numerical solutions of the radiative transfer equations to determine the accuracy of the two-flux method for composites with layers having refractive indices greater than one. The boundaries and interfaces between layers are assumed diffuse.

The Two-Flux and Energy Equations. The two-flux equations used here correspond to the Milne-Eddington

approximation (Sidall, 1972, and Siegel and Howell, 1992). The radiative fluxes q_r^+ and q_r^- are respectively in the positive and negative directions as in Fig. 1; each flux is assumed isotropic. A flux quantity G, and the net radiative flux q_r in the x direction, are related to q_r^+ and q_r^- by,

$$G = 2(q_r^+ + q_r^-) \quad ; \quad q_r = q_r^+ - q_r^- \tag{1a,b}$$

Equations (1a) and (1b) are solved for q_r^+ and q_r^- in terms of G and q_r to give the useful forms,

$$q_r^+ = \frac{1}{2}\left(\frac{G}{2} + q_r\right) \quad ; \quad q_r^- = \frac{1}{2}\left(\frac{G}{2} - q_r\right) \tag{2a,b}$$

The two-flux equations including scattering are given in Siegel and Spuckler (1994) as,

$$\frac{1}{K}\frac{dq_r}{dx} = (1-\Omega)[4n^2\sigma T^4(x) - G(x)] \tag{3}$$

$$\frac{1}{K}\frac{dG}{dx} = -3q_r(x) \tag{4}$$

A third relation, in addition to Eqs. (3) and (4), is the energy equation. For steady state conditions without internal heat sources such as chemical or electrical heating, the heat flow by combined conduction and radiation, q_{tot}, is constant through the composite and is given by,

$$q_{tot} = -k\frac{dT(x)}{dx} + q_r(x) \tag{5}$$

Equations (3), (4) and (5), subject to proper boundary and interface conditions, are to be solved for $q_r(x)$, G(x), and T(x) within the layers of the composite. An iterative solution is used, and the required forms of the equations are now developed.

The $q_r(x)$ in Eq. (5) is eliminated by using Eq. (4). The resulting equation has a first derivative of both T(x) and G(x) and is integrated over x in each of the layers to yield

$$k_j T_j(x_j) = -q_{tot}x_j - \frac{G_j(x_j)}{3K_j} + CON_j \qquad j = 1,2,3 \tag{6}$$

where CON_j is an integration constant in each layer. Evaluating Eq. (6) at $x_j=0$ and $x_j=D_j$ relates the values of q_{tot} and CON_j to the boundary values of T_j and G_j for each layer

$$CON_j = k_j T_j(0) + \frac{G_j(0)}{3K_j} \qquad j = 1,2,3 \tag{7a}$$

$$q_{tot}D_j = -k_j T_j(D_j) - \frac{G_j(D_j)}{3K_j} + CON_j \qquad j = 1,2,3 \tag{7b}$$

Equations (3) and (4), integrated with respect to x_j in each layer, will be used later in the forms,

$$q_{rj}(x_j) = q_{rj}(0) + K_j(1-\Omega_j)\int_0^{x_j}[4n_j^2\,\sigma T_j^4(x_j) - G_j(x_j)]dx_j \quad j = 1,2,3 \tag{8}$$

$$G_j(x_j) = G_j(0) - 3K_j\int_0^{x_j} q_{rj}(x_j)dx_j \qquad j = 1,2,3 \tag{9}$$

Conditions at External Boundaries. The boundary conditions are now developed. Because radiant absorption is a volume process, in the two-flux method there is no absorption at a boundary surface since a surface does not have any volume. Hence at each external boundary of the composite, $x_1 = 0$ and $x_3 = D_3$, convection is balanced by internal heat conduction. Since the total energy flow by radiation and conduction is constant across the entire composite region, the q_{tot} can be expressed at each external boundary as the sum of external convection (which is equal to internal conduction) and internal radiation. This yields at $x_1 = 0$ and $x_3 = D_3$,

$$q_{tot} = h_1[T_{g1} - T_1(0)] + q_{r1}(0) \tag{10a}$$

$$q_{tot} = h_2[T_3(D_3) - T_{g2}] + q_{r3}(D_3) \tag{10b}$$

At each external boundary the radiative flux leaving the internal side of the surface and going into the layer, is equal to the sum of transmitted externally incident flux and reflected internally incident flux. This yields the relations at $x_1 = 0$ and $x_3 = D_3$,

$$q_{r1}^+(0) = (1-\rho_a)q_{r1}^o + \rho_b q_{r1}^-(0) \tag{11a}$$

$$q_{r3}^-(D_3) = (1-\rho_h)q_{r2}^o + \rho_g q_{r3}^+(D_3) \tag{11b}$$

Equations (2a,b) are used to eliminate the q_{r1}^+ and q_{r3}^- from Eqs. (11a,b) to obtain expressions for $G_1(0)$ and $G_3(D_3)$ in terms of the radiative fluxes $q_{r1}(0)$ and $q_{r3}(D_3)$ inside the composite at the boundaries,

$$G_1(0) = 4\frac{1-\rho_a}{1-\rho_b}q_{r1}^o - 2\frac{1+\rho_b}{1-\rho_b}q_{r1}(0) \tag{12a}$$

$$G_3(D_3) = 4\frac{1-\rho_h}{1-\rho_g}q_{r2}^o + 2\frac{1+\rho_g}{1-\rho_g}q_{r3}(D_3) \tag{12b}$$

Relations at Internal Interfaces. At the interface $x_1 = D_1$ ($x_2 = 0$) between layers 1 and 2, the q^+ and q^- are related in terms of transmitted and reflected energy by,

$$q_{r1}^-(D_1) = (1-\rho_d)q_{r2}^-(0) + \rho_c q_{r1}^+(D_1) \tag{13a}$$

At this interface there is also continuity of radiative flux and temperature so that,

$$q_{r1}(D_1) = q_{r2}(0) \quad ; \quad T_1(D_1) = T_2(0) \tag{13b,c}$$

Equations (2a,b) are used to eliminate q^+ and q^- from Eq. (13a) and (13b) is then used to eliminate $q_{r2}(0)$ to give,

$$G_2(0) = \frac{1-\rho_c}{1-\rho_d}G_1(D_1) - 2\frac{\rho_c+\rho_d}{1-\rho_d}q_{r1}(D_1) \tag{14a}$$

Similarly at the second internal interface $x_2 = D_2$ ($x_3 = 0$),

$$G_3(0) = \frac{1-\rho_e}{1-\rho_f} G_2(D_2) - 2\frac{\rho_e+\rho_f}{1-\rho_f} q_{r2}(D_2) \qquad (14b)$$

Relations for Additional Quantities. A relation for q_{tot} is now obtained. Equation (6) is solved for T_j in each of the layers at the internal interfaces. Then continuity of temperature, as in Eq. (13c), is applied to yield at the two interfaces,

$$-q_{tot}\frac{D_j}{k_j} - \frac{1}{3}\frac{G_j(D_j)}{k_jK_j} + \frac{CON_j}{k_j} = -\frac{1}{3}\frac{G_{j+1}(0)}{k_{j+1}K_{j+1}} + \frac{CON_{j+1}}{k_{j+1}} \qquad j = 1,2 \qquad (15)$$

Equation (15) is written for j = 1 and 2, and the two equations are added to eliminate CON_2. Equation (7a) for j = 1 and Eq. (7b) for j = 3 are respectively combined with Eqs. (10a) and (10b) to eliminate the unknown surface temperatures $T_1(0)$ and $T_3(D_3)$. The resulting two equations are combined with Eq. (15) to eliminate CON_1 and CON_3. The expression obtained is solved for q_{tot}, the total heat flow by combined conduction and radiation,

$$q_{tot} = \frac{\sum_{j=1}^{3}\left[\frac{G_j(0)-G_j(D_j)}{3k_jK_j}\right] + T_{g1} - T_{g2} + \frac{q_{r1}(0)}{h_1} + \frac{q_{r3}(D_3)}{h_2}}{\frac{1}{h_1} + \sum_{j=1}^{3}\frac{D_j}{k_j} + \frac{1}{h_2}} \qquad (16)$$

When the correct solution is reached in the iterative method, the change in G across the entire composite, $G_1(0) - G_3(D_3)$ as given by Eqs. (12a,b), should equal the sum of the changes in G across each of the layers as calculated from the integral in Eq. (9) and the change across each of the internal interfaces as obtained from Eqs. (14a) and (14b). To enforce this overall condition during the iterative solution the $q_{rj}(x_j)$ in all of the layers are normalized at each iteration by dividing by the factor NOR obtained from this condition on G

$$NOR = \frac{3\sum_{j=1}^{3} C_jK_j\int_0^{D_j} q_{rj}(x_j)dx_j + 2\frac{\rho_e+\rho_d}{1-\rho_d}\frac{1-\rho_e}{1-\rho_f} q_{r1}(D_1) + 2\frac{\rho_e+\rho_f}{1-\rho_f} q_{r2}(D_2)}{C_1G_1(0) - G_3(D_3)} \qquad (17)$$

The C_j coefficients are

$$C_1 = \frac{1-\rho_c}{1-\rho_d}\frac{1-\rho_e}{1-\rho_f}, \quad C_2 = \frac{1-\rho_e}{1-\rho_f}, \quad C_3 = 1.$$

To obtain expressions for the integration constants CON_j, Eqs. (7a) and (10a) are combined to eliminate $T_1(0)$ to obtain for CON_1

$$CON_1 = k_1\left[T_{g1} + \frac{q_{r1}(0) - q_{tot}}{h_1}\right] + \frac{G_1(0)}{3K_1} \qquad (18a)$$

Similarly CON_3 is obtained by eliminating $T_3(D_3)$ from Eqs. (7b) and (10b),

$$CON_3 = q_{tot}D_3 + k_3\left[T_{g2} + \frac{q_{tot} - q_{r3}(D_3)}{h_2}\right] + \frac{G_3(D_3)}{3K_3} \qquad (18b)$$

With CON_1 known from Eq. (18a), an expression for CON_2 is found by using Eq. (7a) for j = 2 and eliminating $T_2(0)$ by noting that it equals $T_1(D_1)$ found from Eq. (7b). This gives,

$$CON_2 = \frac{k_2}{k_1}(CON_1 - q_{tot}D_1) + \frac{k_2}{3}\left[\frac{G_2(0)}{k_2K_2} - \frac{G_1(D_1)}{k_1K_1}\right] \qquad (18c)$$

Solution Procedure by Iteration for a Gray Three-Layer Composite. The previous relations are solved by iteration to obtain the temperature distribution in the composite and the total heat flow. Before carrying out the solution the equations were placed in dimensionless form using the dimensionless parameters and variables in the Nomenclature. Dimensionless forms are not given here as they somewhat duplicate the previous relations. Some dimensionless forms are given in the next section for a spectral two-band solution.

The iterative solution (given in terms of dimensionless quantities) begins by guessing values of the dimensionless radiative fluxes $\tilde{q}_{rj}(X_j)$ for j = 1,2,3. Using $\tilde{G}_1(0)$ and $\tilde{G}_3(1)$ calculated from Eqs. (12a,b), the $\tilde{q}_{rj}(X_j)$ are normalized by dividing by NOR from Eq. (17). The $\tilde{G}_1(X_1)$ distribution is then obtained from Eq. (9); this also gives $\tilde{G}_1(1)$. Using $\tilde{G}_1(1)$, the $\tilde{G}_2(0)$ is obtained from (14a), and the $\tilde{G}_2(X_2)$ distribution is calculated from Eq. (9). The change in $\tilde{G}$ across the second internal interface is found from Eq. (14b), and $\tilde{G}_3(X_3)$ evaluated from Eq. (9). The $\tilde{q}_{tot}$ is calculated from Eq. (16), and the $\tilde{CON}_j$ for j = 1,2,3 are found from Eqs. (18a,b,c). The $t_j(X_j)$ for j = 1,2,3 are evaluated from Eq. (6). New $\tilde{q}_{rj}(X_j)$ are obtained from Eq. (8) using the starting condition in each successive layer that $\tilde{q}_r$ at the beginning of that layer equals $\tilde{q}_r$ calculated at the end of the previous layer.

To begin a new iteration a damping factor is applied between the new and old $\tilde{q}_{rj}(X_j)$ to keep the iterative method stable. A small damping factor, such as 0.001, is needed; less damping is required in layers with scattering. Computing time for a solution converged to a relative error of 10^{-4} depends on the integration method used in Eqs. (8) and (9). Solutions using the trapezoidal rule took less than 6 seconds on a VAX computer. The numerical solution of the radiative transfer equations using a modified program from Spuckler and Siegel (1994) required at least 12 times more computing time.

Surface reflections were modeled by using integrated averages of the Fresnel reflection relations. For diffuse incidence this gives (Siegel and Howell, 1992, p. 115),

$$\rho(n) = R(n) = \frac{1}{2} + \frac{(3n+1)(n-1)}{6(n+1)^2} + \frac{n^2(n^2-1)^2}{(n^2+1)^3}\ln\left(\frac{n-1}{n+1}\right) - \frac{2n^3(n^2+2n-1)}{(n^2+1)(n^4-1)} + \frac{8n^4(n^4+1)}{(n^2+1)(n^4-1)^2}\ln(n) \qquad n = n_h/n_s \qquad (19)$$

Equation (19) is for reflection by a material with higher refractive index; n_h and n_s are the "higher" and "smaller" n values (incident radiation is from within the n_s material). Allowing for energy incident at directions larger than the angle for total reflection, the $\rho(n)$ for diffuse radiation propagating from a higher to a smaller refractive index material is found from Richmond (1963),

$$\rho(n) = 1 - \frac{1}{n^2}[1 - R(n)] \qquad n = n_h/n_s \qquad (20)$$

Two-Flux Method for Two Spectral Bands in Each Layer of a Two-Layer Composite

A two-band calculation in each layer is used to illustrate the spectral application of the two-flux method for a two-layer composite. The S and L designate bands with small and large frequencies. For a quantity such as $G_\nu(x,\nu)$ the band notation is

$$GS(x) = \int_0^{\nu_c} G_\nu(x,\nu)d\nu \quad ; \quad GL(x) = \int_{\nu_c}^{\infty} G_\nu(x,\nu)d\nu$$

For a two-band calculation each of Eqs. (12) has two parts, one for each frequency range. For example, Eq. (12a) in dimensionless form gives in the small and large frequency ranges,

$$\tilde{G}S_1(0) = 4\frac{1-\rho_a}{1-\rho_b}\tilde{q}S^{\circ}_{r1} - 2\frac{1+\rho_b}{1-\rho_b}\tilde{q}S_{r1}(0) \qquad (21a)$$

$$\tilde{G}L_1(0) = 4\frac{1-\rho_a}{1-\rho_b}\tilde{q}L^{\circ}_{r1} - 2\frac{1+\rho_b}{1-\rho_b}\tilde{q}L_{r1}(0) \qquad (21b)$$

where the ρ are independent of ν. Similar relations are written from Eq. (12b) for $\tilde{G}S_2(1)$ and $\tilde{G}L_2(1)$ at the outer boundary of the second layer. Equation (16) for $\tilde{q}_{tot}$ contains a contribution from each of the two bands, so for a two-layer composite

$$q_{tot} = \left(\frac{1}{H_1} + \sum_{j=1}^{2}\frac{1}{N_j} + \frac{1}{H_2}\right)^{-1}\left\{\sum_{j=1}^{2}\left[\frac{\tilde{G}S_j(0)-\tilde{G}S_j(1)}{3N_j\kappa_{D_jS}} + \frac{\tilde{G}L_j(0)-\tilde{G}L_j(1)}{3N_j\kappa_{D_jL}}\right] + 1 - t_{g2} + \frac{\tilde{q}S_{r1}(0)+\tilde{q}L_{r1}(0)}{H_1} + \frac{\tilde{q}S_{r2}(1)+\tilde{q}L_{r2}(1)}{H_2}\right\} \qquad (22)$$

This also occurs in Eq. (6) for the temperature distribution in each layer,

$$t_j(X_j) = \frac{1}{N_j}\left[-\frac{\tilde{G}S_j(X_j)}{3\kappa_{D_jS}} - \frac{\tilde{G}L_j(X_j)}{3\kappa_{D_jL}} - \tilde{q}_{tot}X_j + C\tilde{O}N_j\right] \quad j = 1,2 \qquad (23)$$

Equation (8) for the radiative flux is written for each band in each layer. For the band with small frequencies in either layer (j = 1,2),

$$\tilde{q}S_{rj}(X_j) = \tilde{q}S_{rj}(0) + \kappa_{D_jS}(1-\Omega_{Sj})\int_0^{X_j}[4n_j^2t_j^4(X_j)FS(X_j) - \tilde{G}S_j(X_j)]dX_j \qquad (24)$$

The $\tilde{q}L_{rj}(X_j)$ for the large frequency band is similar. The $FS(X_j)$ is the fraction of blackbody emission in the small frequency range corresponding to the temperature $T_j(x_j) = t_j(X_j)T_{gl}$.

The change in $\tilde{G}$ when crossing the internal interface is written for each of the bands. For example for the small frequency range, from Eq. (14a),

$$\tilde{G}S_2(0) = \frac{1-\rho_c}{1-\rho_d}\tilde{G}S_1(1) - 2\frac{\rho_o+\rho_d}{1-\rho_d}\tilde{q}S_{r1}(1) \qquad (25)$$

The normalization factor in Eq. (17) is written for a two layer composite in each of the bands. For the small frequency band,

$$NORS = \frac{3\frac{1-\rho_o}{1-\rho_d}\kappa_{D_1S}\int_0^1\tilde{q}S_{r1}(X_1)dX_1 + 3\kappa_{D_2S}\int_0^1\tilde{q}S_{r2}(X_2)dX_2 + 2\frac{\rho_o+\rho_d}{1-\rho_d}\tilde{q}S_{r1}(1)}{\frac{1-\rho_o}{1-\rho_d}\tilde{G}S_1(0) - \tilde{G}S_2(1)} \qquad (26)$$

The integration constants in Eq. (18) are written in each of the two layers as (including contributions from both bands),

$$C\tilde{O}N_1 = N_1\left[1 + \frac{\tilde{q}S_{r1}(0)+\tilde{q}L_{r1}(0)-\tilde{q}_{tot}}{H_1}\right] + \frac{\tilde{G}S_1(0)}{3\kappa_{D_1S}} + \frac{\tilde{G}L_1(0)}{3\kappa_{D_1L}} \qquad (27a)$$

$$C\tilde{O}N_2 = \tilde{q}_{tot} + N_2\left[t_{g2} - \frac{\tilde{q}S_{r2}(1)+\tilde{q}L_{r2}(1)-\tilde{q}_{tot}}{H_2}\right] + \frac{\tilde{G}S_2(1)}{3\kappa_{D_2S}} + \frac{\tilde{G}L_2(1)}{3\kappa_{D_2L}} \qquad (27b)$$

The solution by iteration follows the same steps outlined for gray layers except there are now two $q_r(X)$ in each layer, one for each spectral band. Following the procedure for the gray case, calculations are made in each band. The bands contribute to the temperature as given by Eq. (23). The iteration begins by estimating $qS_r(X)$ and $qL_r(X)$ for each band by taking into account that $q_r(X)$ tends to be small in a band where κ_D is large, and that the radiative energy distribution in the bands shifts to smaller ν as $t(X)$ decreases. Converged solutions for the two-flux method using the trapezoidal rule for integration required up to 5 minutes on a VAX computer. The exact numerical solution required about twice that time or longer.

Two-Layer Solution Using the Two-Flux Method in the First Layer and the Diffusion Method in the Second Layer

When the optical thickness of a layer is large, the radiative diffusion method is very useful for making predictions for either a gray or spectral layer (Siegel and Spuckler, 1994). A two-layer geometry is considered here with an optical thickness of about 20 or less in each of the bands of the first layer, and with a larger optical thickness in the second layer. The two-flux method is used in the first layer for both spectral bands. The second layer is gray and is analyzed with the diffusion method. The analysis shows how the two-flux method is joined with a diffusion solution. The required relations draw upon the previous two-flux analysis, but there are several new features.

The first step in the iterative solution is to use Eqs. (21a,b) to calculate $\tilde{G}S_1(0)$ and $\tilde{G}L_1(0)$ at the outer boundary of the first layer for each of the spectral bands. The radiative energy balance at the first surface of the second layer, $X_1 = 1$, is then used to obtain relations for $\tilde{G}S_1(1)$ and $\tilde{G}L_1(1)$. Since the second layer is gray with radiative diffusion this balance gives,

$$\tilde{q}^-_{r1}(1) = (1-\rho_c)n_1^2t_2^4(0) + \rho_c\tilde{q}^+_{r1}(1) \; .$$

Equations (2a,b) are used to eliminate $\tilde{q}^-$ and $\tilde{q}^+$ and the result is written for each band to give,

$$\tilde{G}S_1(1) = 4n_1^2t_2^4(0)FS[t_2(0)T_{gl}] + 2\frac{1+\rho_c}{1-\rho_c}\tilde{q}S_1(1) \qquad (28a)$$

$$\tilde{G}L_1(1) = 4n_1^2 t_2^4(0) FL[t_2(0)T_{g1}] + 2\frac{1+\rho_e}{1-\rho_e}\tilde{q}L_1(1) \qquad (28b)$$

where the FS and FL are blackbody fractions that depend on the temperatures shown and on the cutoff frequency of the bands. Equations (28a,b) depend on the interface temperature $t_2(0)$ which is an unknown; hence the $\tilde{G}S_1(1)$ and $\tilde{G}L_1(1)$ must be determined simultaneously with Eqs. (29a,b,c) that follow.

A set of three simultaneous equations is now developed. In a similar manner to Eq. (22) the two-flux relation for q_{tot} in the first layer is written as

$$\tilde{q}_{tot} = \frac{\dfrac{\tilde{G}S_1(0)-\tilde{G}S_1(1)}{3N_1\kappa_{D_1S}} + \dfrac{\tilde{G}L_1(0)-\tilde{G}L_1(1)}{3N_1\kappa_{D_1L}} + \dfrac{\tilde{q}S_1(0)+\tilde{q}L_1(0)}{H_1} + 1 - t_2(0)}{\dfrac{1}{H_1}+\dfrac{1}{N_1}} \qquad (29a)$$

The combination of conduction and radiative diffusion across the second layer gives a relation for $\tilde{q}_{tot}$ as derived in Siegel and Spuckler (1994),

$$\tilde{q}_{tot} = N_2[t_2(0) - t_2(1)] + \frac{4n_2^2}{3\kappa_{D_2}}[t_2^4(0) - t_2^4(1)] \qquad (29b)$$

The convective and radiative energy balance at the outside boundary $X_2 = 1$ of the second layer gives,

$$\tilde{q}_{tot} = H_2[t_2(1) - t_{g2}] + (1-\rho_e)n_2^2[t_2^4(1) - \tilde{q}^{\circ}_{r2}] \qquad (29c)$$

Using Eqs. (28a,b) as constraints, Eqs. (29a,b,c) are solved simultaneously for the interface and boundary temperatures $t_2(0)$, and $t_2(1)$, of the diffusion layer, and the heat flow $\tilde{q}_{tot}$ through the composite. The temperature distribution in the second layer is then calculated by solving Eq. (30) numerically for $t_2(X_j)$. This was derived in Siegel and Spuckler (1994) by using radiative diffusion in the energy equation,

$$t_2(X_2) - t_2(1) + \frac{4n_2^2}{3N_2\kappa_{D_2}}[t_2^4(X_2) - t_2^4(1)] = \frac{\tilde{q}_{tot}(1-X_2)}{N_2} \qquad (30)$$

Converged solutions using the trapezoidal rule required less than 1 minute on a VAX computer; exact numerical solutions took about 20 times longer.

RESULTS AND DISCUSSION

The two-flux method was developed in Siegel and Spuckler (1994) for a single gray layer with refractive index $n > 1$ and external convective and radiative conditions. Excellent agreement was found with numerical solutions of the exact radiative transfer equations. The two-flux method is further developed here for multiple layers that are either gray or have two spectral bands in each layer. An extension is also made to generalize the results for the radiative boundary condition on the hot side of the composite. The incident radiative flux on the hot side is $q^{\circ}_{r1} = \sigma T^4_{s1}$ which is the flux from blackbody surroundings with an effective temperature T_{s1}. In Siegel and Spuckler (1994) the results are for $T_{s1} = T_{g1}$ where T_{g1} is the temperature of the gas providing convective heating or cooling on the hot side at $x_1 = 0$. In the results that follow, the T_{s1} can be greater or less than T_{g1}. This shows the effect of the gas either cooling or heating the surface relative to the radiative energy being supplied.

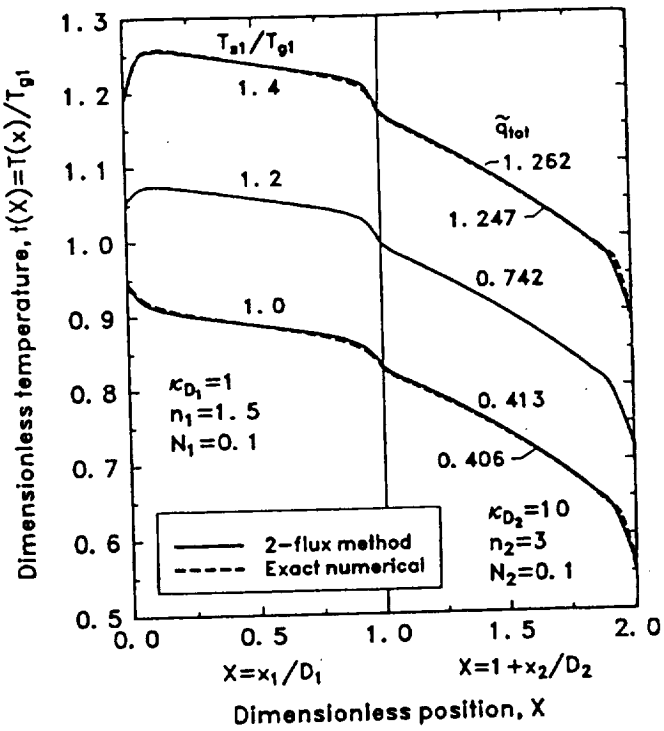

FIG. 2 TWO-FLUX RESULTS IN COMPOSITE OF TWO GRAY LAYERS SHOWING EFFECT OF A RADIATIVE HOT SIDE SURROUNDING TEMPERATURE DIFFERENT FROM THE GAS TEMPERATURE. COMPARISONS ARE SHOWN WITH NUMERICAL SOLUTIONS: $n_1 = 1.5$, $n_2 = 3$, $\tilde{q}^{\circ}_{r1} = 1.0^4 - 1.4^4$, $\tilde{q}^{\circ}_{r2} = 0.25^4$, $t_{g1} = 1$, $t_{g2} = 0.25$, $H_1 = H_2 = 1$, $N_1 = N_2 = 0.1$.

Two-Flux Results for a Composite of Two Gray Layers

Figure 2 shows two-flux results for a two-layer composite with the first and second layers having optical thicknesses of 1 and 10 and refractive indices of 1.5 and 3. The first layer, that is exposed to the radiation on the hot side, is somewhat optically thin. For the results shown T_{s1}/T_{g1} is 1.0, 1.2 and 1.4. For $T_{s1}/T_{g1} = 1.2$ and 1.4 there is sufficient radiative absorption within the first layer that the temperature is a maximum within that layer. Some of the absorbed radiation is being removed by convection at the boundaries. This results in a large temperature change near the boundary that can produce thermal stresses. For $T_{s1}/T_{g1} = 1$ the gas temperature is the same as the radiative surroundings and the temperature gradient is reversed at the hot surface. This is the result of cooling by radiation and conduction through the entire composite by the lower temperature gas and environment at the outside boundary of the second layer.

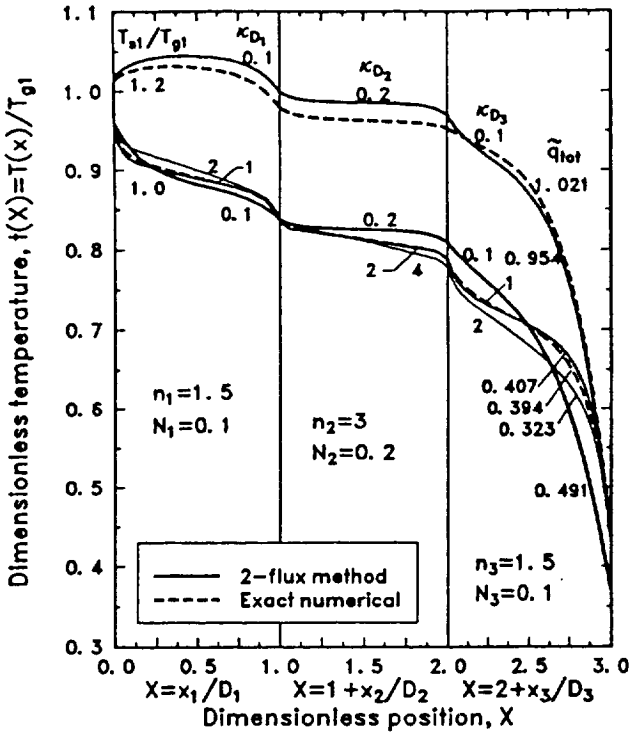

FIG. 3 COMPARISONS OF TWO-FLUX RESULTS WITH EXACT NUMERICAL SOLUTIONS OF TRANSFER EQUATIONS FOR COMPOSITE OF THREE GRAY LAYERS: $n_1 = n_3 = 1.5$, $n_2 = 3$, $\tilde{q}^{\circ}_{r1} = 1$ and 1.2^4, $\tilde{q}^{\circ}_{r2} = 0.25^4$, $t_{g1} = 1$, $t_{g2} = 0.25$, $H_1 = H_2 = 1$, $N_1 = N_3 = 0.1$, $N_2 = 0.2$.

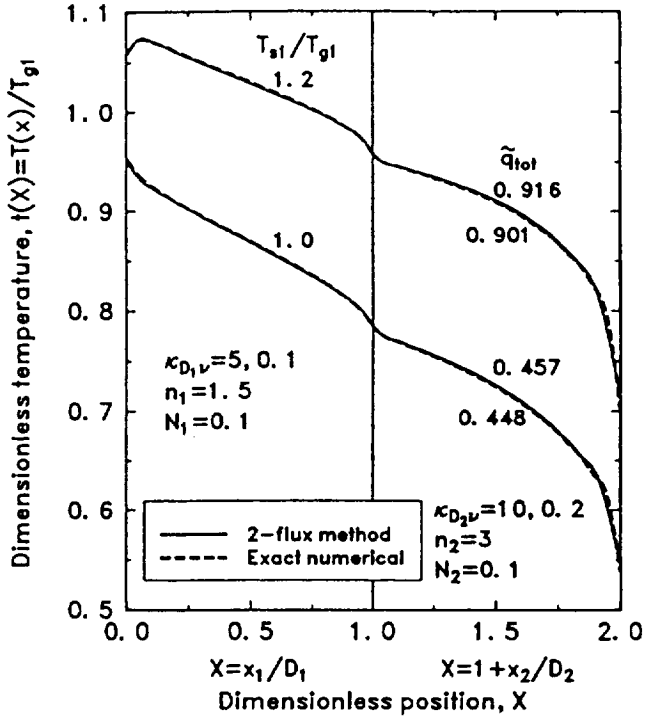

FIG. 4 TWO-FLUX RESULTS IN COMPOSITE OF TWO LAYERS, EACH WITH TWO SPECTRAL BANDS. EFFECT OF HOT SIDE SURROUNDINGS TEMPERATURE DIFFERENT FROM THE GAS. COMPARISONS WITH NUMERICAL SOLUTIONS. OPTICAL THICKNESS OF BANDS IN ORDER OF INCREASING FREQUENCY: $a_{\nu 1}D_1 = 5$, 0.1, $a_{\nu 2}D_2 = 10$, 0.2 and cutoff frequency, $\nu_c/c_0T_{g1} = 1/4000$; $n_1 = 1.5$, $n_2 = 3$, $\tilde{q}^{\circ}_{r1} = 1$ and 1.2^4, $\tilde{q}^{\circ}_{r2} = 0.25^4$, $t_{g1} = 1$, $t_{g2} = 0.25$, $H_1 = H_2 = 1$, $N_1 = N_2 = 0.1$.

For some of the cases comparisons are shown with "exact" numerical solutions of the radiative transfer equations using the computer program of Spuckler and Siegel (1994). Very good agreement is obtained for the temperature distributions and the total heat flux by combined radiation and conduction. The two-flux method yields good predictions for a composite of two layers and for conditions when there is large incident radiation.

Two-Flux Results for a Composite of Three Gray Layers

Figure 3 shows results for a composite of three gray layers with n = 1.5 in layers 1 and 3, and n = 3 in layer 2. The optical thicknesses range from 0.1 to 2 in layers 1 and 3, and from 0.2 to 4 in layer 2. The "exact" numerical results were obtained by extending the computer program of Spuckler and Siegel (1994) to three-layers. As shown by the lower set of curves, that are for three different levels of optical thickness, the two-flux method yields good temperature predictions when κ_D in each layer is of order one. The two-flux results follow the pronounced temperature curvature near the boundaries and the internal interfaces. There is a little more deviation from the numerical solution when the optical thicknesses are small as shown by the two uppermost curves on the figure that are for $T_{s1}/T_{g1} = 1.2$. The heat flux through the layer by combined radiation and conduction is predicted within 7% by the two-flux method as shown by the values on the figure.

Two-Flux Results for a Two-Layer Composite with Two Spectral Bands in each Layer

For the results in Fig. 4 the spectral absorption coefficient has two bands in each of the layers: for small ν, $\nu_c/c_0T_{g1} < 1/4000$, $a_{\nu S}D_1 = 5$ and $a_{\nu S}D_2 = 10$, while for large ν, $\nu_c/c_0T_{g1} > 1/4000$, $a_{\nu L}D_1 = 0.1$ and $a_{\nu L}D_2 = 0.2$. The selected value of the cutoff frequency ν_c divides the blackbody spectrum at T_{g1} into approximately two equal parts. The $N_1 = N_2$, and is the same as on Fig. 2, and the temperature ratio T_{s1}/T_{g1} is 1 and 1.2. The temperature distributions show the same general trends that were discussed for gray layers in Fig. 2. For the two-band calculations the temperature distribution and total heat flux results from the two-flux method compare very well with the numerical solutions of the radiative transfer equations. The two-flux predictions of the total heat flux are within about 2% of the numerical solution.

Results for a Two-Layer Composite with Two-Flux Method in the First Layer and Diffusion in the Second Layer

In Fig. 5a the two layers are gray with $a_1D_1 = 1$ and $a_2D_2 = 100$. The diffusion method can be applied with good accuracy in the second layer. Temperature profiles are shown for T_{s1}/T_{g1} in the range 0.8 to

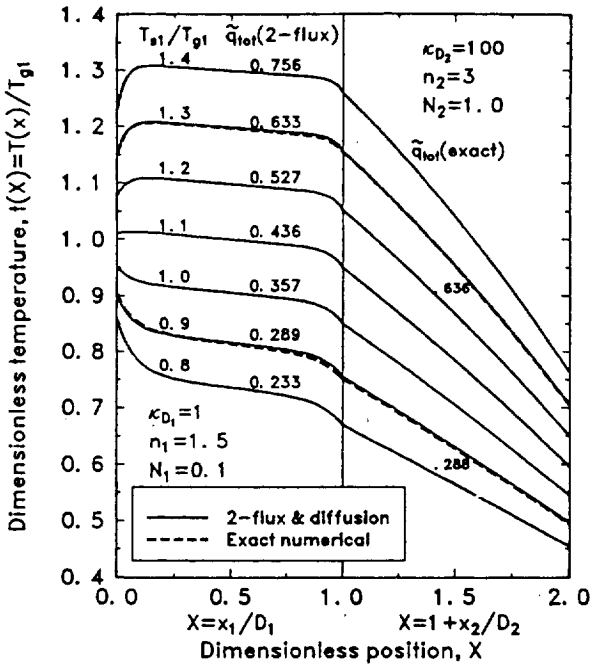

(a)

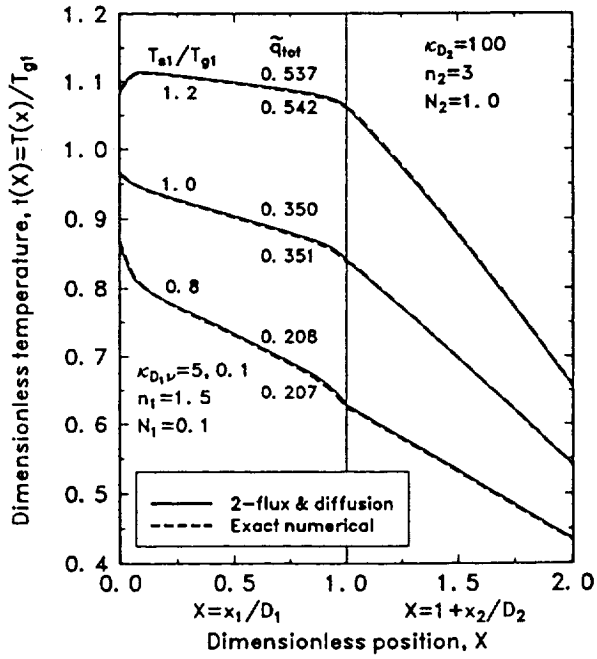

(b)

FIG. 5 TEMPERATURE DISTRIBUTIONS SHOWING EFFECTS OF SURROUNDINGS TEMPERATURE USING COMBINED TWO-FLUX AND DIFFUSION METHODS FOR TWO-LAYERS: $n_1 = 1.5$, $n_2 = 3$, $\bar{q}^{\circ}_{r1} = 0.8^4 - 1.4^4$, $\bar{q}^{\circ}_{r2} = 0.25^4$, $t_{g1} = 1$, $t_{g2} = 0.25$, $H_1 = H_2 = 1$, $N_1 = 0.1$, $N_2 = 1$.
(a) BOTH LAYERS ARE GRAY: $a_1D_1 = 1$ and $a_2D_2 = 100$.
(b) FIRST LAYER HAS TWO SPECTRAL BANDS: $a_{\nu 1}D_1 = 5$, $a_{\nu 2}D_2 = 0.1$ with cutoff $\nu_c/c_0T_{g1} = 1/4000$; SECOND LAYER IS GRAY: $a_2D_2 = 100$.

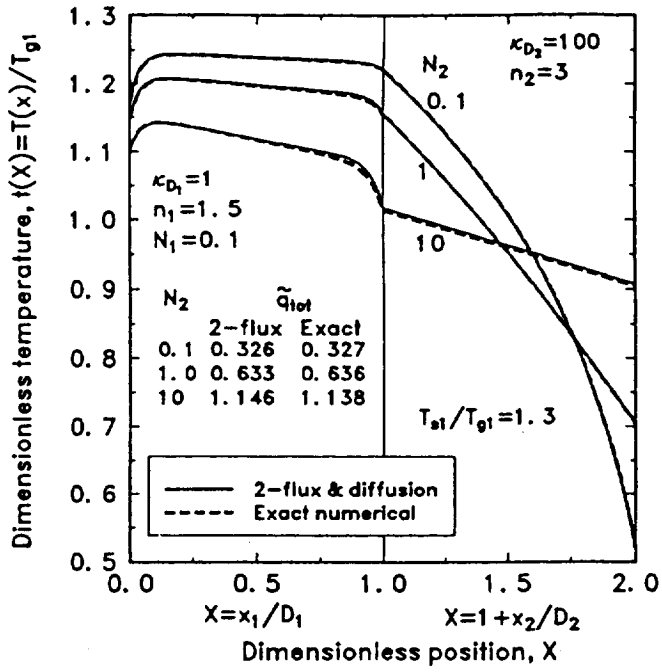

FIG. 6 EFFECT OF THERMAL CONDUCTIVITY IN SECOND LAYER ON TEMPERATURE DISTRIBUTIONS IN TWO GRAY LAYERS USING COMBINED TWO-FLUX AND DIFFUSION ; $n_1 = 1.5$, $n_2 = 3$, $\bar{q}^{\circ}_{r1} = 1.3^4$, $\bar{q}^{\circ}_{r2} = 0.25^4$, $t_{g1} = 1$, $t_{g2} = 0.25$, $H_1 = H_2 = 1$, $N_1 = 0.1$, $N_2 = 0.1$, 1, 10.

1.4. For comparison two cases are given from the numerical solution of the radiative transfer equations; very good agreement is obtained. This, and the ability of the iterative combined two-flux diffusion solutions to converge reasonably well, shows that the two-flux method can be used quite well in layers that are not too optically thick ($\kappa_D <$ ~20), and the solution joined to the diffusion method in an adjacent optically thick layer.

The general behavior of the results in Fig. 5a are similar to those discussed for Fig. 2. Decreasing the temperature ratio T_{s1}/T_{g1} decreases the overall temperature in the layer while the profiles remain similar. There is a change in slope from positive to negative at the hot gas interface when T_{s1}/T_{g1} is about 1.1. For a large optical thickness in the second layer radiative transmission is diminished and conduction has an important effect. This leads to profiles in the second layer that tend to be more linear.

In Fig. 5a both layers are gray; in Fig. 5b results are given for the first layer having two spectral bands so that for small ν, $\nu_c/c_0T_{g1} <$ 1/4000, $a_{\nu S}D_1 = 5$, while for large ν, $\nu_c/c_0T_{g1} >$ 1/4000, $a_{\nu L}D_1 = 0.1$. The selected value of the cutoff frequency ν_c divides the blackbody spectrum at T_{g1} into approximately two equal parts. The results have the same general behavior as in Fig. 5a and the two-flux method is again in good agreement with the numerical solutions of the radiative transfer equations.

The results in Fig. 5a are extended in Fig. 6 to show the effect of changing the thermal conductivity in the second layer. The conduction parameter is $N_2 = 1$ in Fig. 5a, and this is compared in Fig. 6 to results for $N_2 = 0.1$ and 10. A large N_2 enhances conduction through the

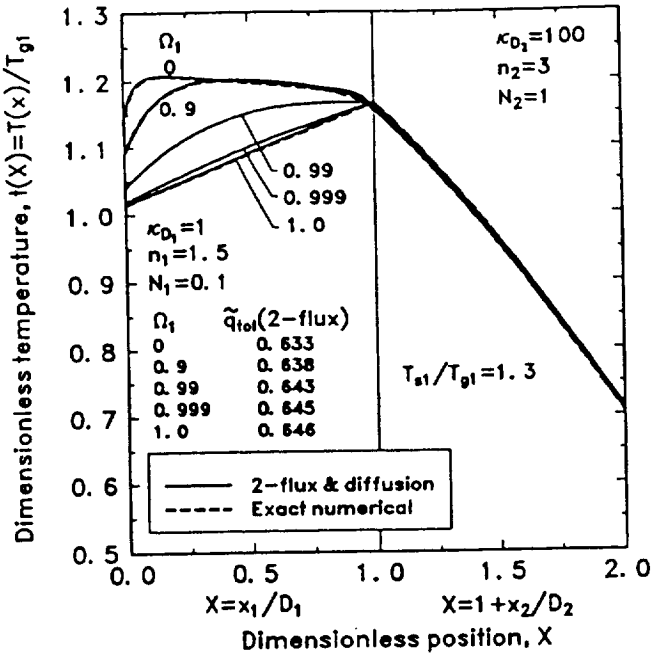

FIG. 7 EFFECT OF SCATTERING ALBEDO ON TEMPERATURE DISTRIBUTIONS FOR COMBINED TWO-FLUX AND DIFFUSION METHODS IN TWO-LAYER COMPOSITE: $n_1 = 1.5$, $n_2 = 3$, $\bar{q}^*_{r1} = 1.3^4$, $\bar{q}^*_{r2} = 0.25^4$, $t_{g1} = 1$, $t_{g2} = 0.25$, $H_1 = H_2 = 1$, $N_1 = 0.1$, $N_2 = 1$.

second layer and results in reduced temperatures in the first layer including a reduced temperature at the surface exposed to the hot environment.

Effect of Scattering in the First Layer of a Two-Layer Composite Using Combined Two-Flux and Diffusion Methods

The results in Figs. 5 and 6 are without any scattering. Figure 7 shows the effect of having large scattering so the scattering albedo Ω_1 is from 0.9 to 1.0 (the limit with no absorption). The results are compared with the case for absorption only, $\Omega_1 = 0$. Since the optical thickness is kept constant, increasing the albedo corresponds to decreased absorption and the temperature profile in the first layer approaches a straight line for conduction only. There is radiation going from the hot side environment through the first layer and then being absorbed at the internal interface; for very large scattering the temperature maximum is then at or near the internal interface. The results show good agreement with numerical solutions of the transfer equations indicating that scattering can be included with good accuracy in the two-flux method.

CONCLUSIONS

The prediction of temperature distributions and heat transfer is carried out in composite semitransparent layers heated on both sides by radiation and convection. The external conditions are such that the boundary temperatures are not specified and must be determined by the solution. The layers in the composite have differing refractive indices that are larger than one, and isotropic scattering is included. Two methods were developed for performing spectral calculations in multilayered composites. The two-flux method was developed for multilayer composites of three layers and was found to give good agreement with exact numerical solutions for all conditions considered. When one layer in a composite is optically thick the theory was developed to use the diffusion method in that layer and join it to the two-flux method used in the other layers. This gives better convergence than using the two-flux method in an optically thick layer.

When the hot surroundings are at a different temperature than the gas on the hot side, there can be large temperature gradients near the hot side surface that can cause thermal stresses. If the hot surroundings are at a higher temperature than the gas on the hot side, the maximum temperature can occur in the interior of the material rather than at the surface. This can be important if the material is operating near its upper temperature limit for adequate strength.

REFERENCES

Gardon, R., 1958, "Calculation of Temperature Distributions in Glass Plates Undergoing Heat-Treatment," *Journal of the American Ceramic Society*, Vol. 41, pp. 200-209.

Malpica, F., Campo. A., and Tremante, A., 1986, "Contribution of Thermal Radiation to the Temperature Profile of Semitransparent Materials," *High Temperatures-High Pressures*, Vol. 18, pp. 35-41.

Richmond, J. C., 1963, "Relation of Emittance to Other Optical Properties," *Journal of Research of the National Bureau of Standards*, Vol. 67C, pp. 217-226.

Sidall, R. G., 1972, "Flux Methods for the Analysis of Radiant Heat Transfer," *Proceedings of the Fourth Symposium on Flames and Industry*, The Institute of Fuel, Paper 16, pp. 169-179.

Siegel, R., and Howell, J. R., 1992, Thermal Radiation Heat Transfer, 3rd edition, Hemisphere, Washington D.C.

Siegel, R., and Spuckler, C. M., 1994, "Approximate Solution Methods for Spectral Radiative Transfer in High Refractive Index Layers," *International Journal of Heat and Mass Transfer*, Vol. 37, Suppl. 1, pp. 403-413.

Spuckler, C. M., and Siegel, R., 1993, "Refractive Index and Scattering Effects on Radiative Behavior of a Semitransparent Layer," *Journal of Thermophysics and Heat Transfer*, Vol. 7, pp. 302-310.

Spuckler, C. M., and Siegel, R., 1994, "Refractive Index and Scattering Effects on Radiation in a Semitransparent Laminated Layer," *Journal of Thermophysics and Heat Transfer*, Vol. 8, pp. 193-201.

Tremante, A., and Malpica, F., 1993, "Contribution of Thermal Radiation to the Temperature Profile of Ceramic Composite Materials," ASME Paper 93-GT-325, International Gas Turbine and Aeroengine Congress and Exposition, Cincinnati, OH, May 24-27, 1993, 6 pp.